

# Preparation and electromagnetic microwave adsorption performances of porous nanocomposite self-assembled by $\text{CoFe}_2\text{O}_4$ nanoparticles and diatomite

**Haodong HUANG**

is a final year student of innovation programme of Resource Recycling in Southwest University of Science and Technology of China under supervision of Prof. Shiyong Sun.

**Meng HE**

is a second year postgraduate student of Geological Resources and Geological Engineering in Southwest University of Science and Technology of China under supervision of Prof. Shiyong Sun.

**Olga B. KOTOVA**

is Head of Laboratory of Technology of Mineral Raw, Institute of Geology Komi SC UB Russian Academy of Sciences. Author and co-author of 10 books, 4 patents and more than 200 scientific articles. President of ICAM-2019. The member of Science Council of Russian Mineralogical Society

**Yevgeny A. GOLUBEV**

is leading researcher of Laboratory of Experimental Mineralogy, Institute of Geology Komi SC UB Russian Academy of Sciences. Author and co-author of 5 books and more than 60 scientific articles. The member of Russian Mineralogical Society.

**Faqin DONG**

is a professor of School of Environment and Resource of Southwest University of Science and Technology of China. He is author or co-author of more than 300 scientific papers.

**László A. GÖMZE**

is establisher and professor of the Department of Ceramics and Silicate Engineering in the University of Miskolc, Hungary. He is author or co-author of 2 patents, 6 books and more than 300 scientific papers.

**Emese KUROVICS**

is graduated from the University of Miskolc, Department of Ceramics and Silicate Engineering as a material engineer, where she continues her study as PhD student under supervision of Prof. L. A. Gömze.

**Rui LV**

is a second year PhD student of Environment Science and Technology in Southwest University of Science and Technology of China under supervision of Prof. Shiyong Sun.

**Shiyong SUN**

is a professor of School of Environment and Resource of Southwest University of Science and Technology of China. He is author or co-author of more than 80 scientific papers.

**HAODONG HUANG** • Key Laboratory of Solid Waste Treatment and Resource Recycle of Ministry of Education, School of Environment and Resource, Southwest University of Science and Technology, China

**MENG HE** • Key Laboratory of Solid Waste Treatment and Resource Recycle of Ministry of Education, School of Environment and Resource, Southwest University of Science and Technology, China

**OLGA B. KOTOVA** • Institute of Geology, Komi Science Center, Ural Branch of the Russian Academy of Sciences, Russian Federation

**YEVGENY GOLUBEV** • Institute of Geology, Komi Science Center, Ural Branch of the Russian Academy of Sciences, Russian Federation

**FAQIN DONG** • Key Laboratory of Solid Waste Treatment and Resource Recycle of Ministry of Education, School of Environment and Resource, Southwest University of Science and Technology, China

**LÁSZLÓ A. GÖMZE** • Institute of Ceramics and Polymer Engineering, University of Miskolc, Miskolc, Hungary, IGREX Engineering Service Ltd

**EMESE KUROVICS** • Institute of Ceramics and Polymer Engineering, University of Miskolc, Hungary

**RUI LV** • Key Laboratory of Solid Waste Treatment and Resource Recycle of Ministry of Education, School of Environment and Resource, Southwest University of Science and Technology, China

**SHIYONG SUN** • Key Laboratory of Solid Waste Treatment and Resource Recycle of Ministry of Education, School of Environment and Resource, Southwest University of Science and Technology, China  
▪ shysun@swust.edu.cn

Érkezett: 2020. 06. 30. • Received: 30. 06. 2020. • <https://doi.org/10.14382/epitoanyag-jsbcm.2020.20>

## Abstract

The efficient nanocomposite of  $\text{CoFe}_2\text{O}_4$  diatomite for electromagnetic microwave adsorption was assembled by  $\text{CoFe}_2\text{O}_4$  nanoparticles (NPs) and diatomite via a simple citric acid-nitrate sol-gel auto-combustion method. The electronic microscopy results show that the magnetic  $\text{CoFe}_2\text{O}_4$  NPs are uniformly dispersed in the surface and porous structure of diatomite to form stable  $\text{CoFe}_2\text{O}_4$ /diatomite nanocomposite. The magnetic and dielectric properties with various mass ratios of  $\text{CoFe}_2\text{O}_4$  to diatomite was investigated. It was showed that nanocomposite of  $\text{CoFe}_2\text{O}_4$ /diatomite has strong superparamagnetic and electromagnetic microwave absorbing properties with optimized conditions of coercive force of 837.07 Oe, the saturation magnetization of 96.5 emu/g, and the remanence ratio (Mr/Ms) of 0.52, respectively. The maximum reflection loss is -12dB, and <10dB frequency ranges from 10Hz to 12Hz when the ratio of  $\text{CoFe}_2\text{O}_4$  to Diatomite is 1:10. The results indicate that  $\text{CoFe}_2\text{O}_4$ /diatomite composites can be used as the highly efficient microwave absorption materials, which expanded the application field of diatomite-based functional nanomaterials.

Keywords: diatomite;  $\text{CoFe}_2\text{O}_4$ , electromagnetic microwave adsorbent, nanocomposite, porous minerals

Kulcsszavak: kovaföld,  $\text{CoFe}_2\text{O}_4$ , elektromágneses mikrohullámú adszorbens, nanokompozitot, porózus ásványok

## 1. Introduction

With the rapid development of electronic technologies, the electromagnetic interference (EMI) caused by electromagnetic microwaves (EMW) is becoming serious problems. The harmful electromagnetic radiation (EM radiation or EMR) not only affects sensitive electronic equipment, but also harmful to human health [1, 2]. In order to reduce the impact of EMW, scientists pay much attention to explore and design high-performance electromagnetic wave absorbing materials with properties of lightweight, wide frequency range and low cost [3-7]. The EM absorbing material has been applied not only

in the stealth technology of military, but also the ordinary commercial productions in all aspects to effectively reduce the reflection and transmission of EMW by converting EM into thermal energy [7-9]. Generally, the typical electromagnetic wave adsorbents are constructed by embedding an EMW adsorbent into a host matrix, whose microwave adsorbing properties are primarily determined by the suspended materials.

Ferrite is one of the main frequently used microwave absorbing materials, which can efficiently absorb harmful electromagnetic radiation [10, 11]. Spinel ferrite ( $MFe_2O_4$ ,  $M = Mn, Mg, Co, Cu, Zn, Ni, Fe$  etc.) exhibits adjustable saturation magnetization, excellent chemical stability, low real dielectric constant and high magnetic loss. Among these spinel ferrites,  $CoFe_2O_4$  received particular attention due to their remarkable properties, which include a moderate saturation magnetization, excellent chemical stability, and high mechanical hardness [12]. On the basis of these characteristics,  $CoFe_2O_4$  ferrite can be used as a powerful EMW adsorption material [13]. However, bulk magnet  $CoFe_2O_4$  ferrite has disadvantages of high density, narrow bandwidth and large absorber thickness, which restricted their applications. In order to overcome these disadvantages and improve its adsorbing efficiency, one effective strategy is to immobilize ferrite nanoparticles (NPs) on high physical and chemical stability porous supports such as activated carbon [14], silica [15, 16] and graphene [17, 18], which realized to wide absorbing band (below -10 dB), lightweight, corrosion resistance and high temperature resistance [3, 19-21].

Diatomite is a low-cost silicate mineral composed by silica microfossils of aquatic algae with high permeability and porous structure that possesses the properties of large surface area, small particle size, and remarkable thermal stability [22, 23]. Therefore, diatomite is one of the most promising supports for dielectric materials [9, 24], which explored for preparation of EMW adsorbing nanocomposite. It has technical challenges for general utilization of the coal-derived diatomite due to its high contents of organic matters and iron in diatomite industrial of China. Thus, the large-scale sustainable utilization of coral-derived diatomite as a porous support for preparation of EMW adsorbing materials was taken into consideration. In the presented work, the  $CoFe_2O_4$ /diatomite nanocomposite for EMW adsorbing was prepared by citric acid-nitrate sol-gel auto-combustion method using coal-derived diatomite as support. The electromagnetic properties of the as-prepared nanocomposites were studied in the frequency range of 0~18GHz.

## 2. Materials and methods

### 2.1 Materials

The experimental used diatomite is the purified from the Xianfeng coal mine of China.  $CoCl_2 \cdot 6H_2O$  of analysis grade was purchased from the pharmaceutical group of chemical reagents;  $FeCl_3 \cdot 6H_2O$ , PVP, NaOH, and anhydrous ethanol were obtained from Chengdu Kelon Chemical Reagent company. All other chemicals or reagents were used without further purification.

## 2.2 Preparation of $CoFe_2O_4$ /diatomite nanocomposite

### 2.2.1 Purification of diatomite

Generally, 250 g of diatomite was added into water to prepare aqueous suspension with water-diatomite ratio of about 20:1 (water depth: 40 cm). Then, the upper aqueous layer of 5 cm was taken out after stirring at a suitable speed (300 rpm) for 30 min. The remaining sample was centrifuged to obtain pellets of purified diatomite. The wet pellets of purified diatomite was dried by common muffle furnace at 70 °C for experiments.

### 2.2.2 Preparation of $CoFe_2O_4$ NPs

For sintering was chosen based on the  $SiO_2$ - $Al_2O_3$  phase diagram [17], waiting for the following phase transitions: 450 °C – kaolinite–metakaolinite; 575 °C.

### 2.2.3 Preparation of nanocomposite

The purified diatomite was added into above mentioned first preparation process of  $CoFe_2O_4$  NPs for preparation of suspension with various ratios. The as-prepared samples after auto-combustion process was homogenous dispersed into ethanol, and then ultrasonic treated 20 min and shaken at room temperature for 5h. The as-prepared samples were finally dried in a vacuum oven at room temperature overnight for characterization. Finally, the nanocomposite samples were calcined at different temperatures for 2 h in muffle furnace.

## 2.3 Characterization

The mineral phase characterization was carried out using X'Pert Pro X-ray diffractometer (XRD) from PANalytical, Netherlands. The ULTRA55 field emission scanning electron microscopy (FE-SEM) and Libra 200FE-type transmission electron microscopy (TEM) were used to observe the morphological characteristics. The magnetic characterizations were carried out using the BKT-4500Z high precision vibration sample magnetometer of Beijing Xinke GaoShan Technology Co., Ltd. An Agilent N5230C microwave network analyzer was used to analyze the microwave absorption characteristics of the material.

## 3. Results and discussions

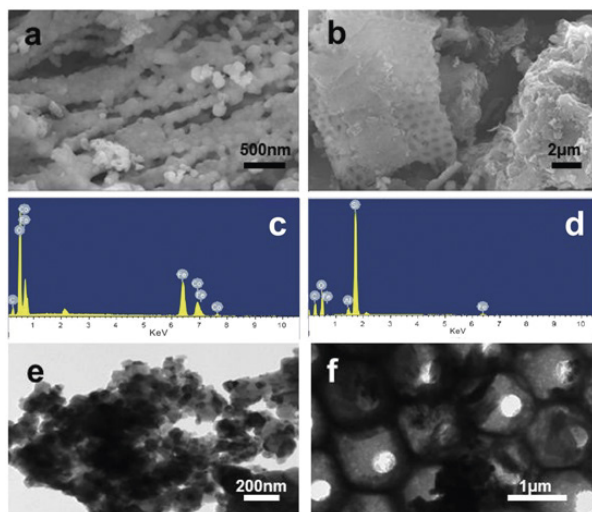
### 3.1 Morphological observations

The FE-SEM and TEM were used for characterizing the morphology of samples. Micrographs show the formation of spherical  $CoFe_2O_4$  NPs with average particle size of 40 nm (Fig. 1a, 1e). As shown in Figures 1b and 1f, the distinctive porous structures of the diatomite were occupied by  $CoFe_2O_4$  NPs. The elemental components of  $CoFe_2O_4$  NPs and  $CoFe_2O_4$ /diatomite nanocomposite (DCNC) were identified by EDX analysis (Fig. 1c, 1d). The EDX patterns qualitatively confirmed the presence of Co, Fe and O in the DCNC.

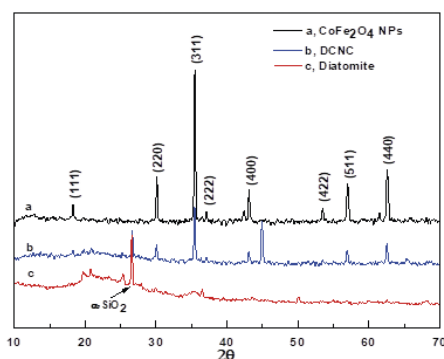
### 3.2 XRD characterization

The XRD characteristics of  $CoFe_2O_4$  NPs, DCNC and diatomite are shown in Fig. 2. The diffraction peaks appeared at Bragg angles  $2\theta$  ~ 18.3°, 30.1°, 35.4°, 37.1°, 43.1°, 53.4°, 57.0°

and 62.6° corresponding to (111), (220), (311), (222), (400), (422), (511) and (440) planes of  $\text{CoFe}_2\text{O}_4$ , respectively with  $a=b=c=8.377$ , by which confirmed the formation of cubic spinel structure. The natural diatomite is in the amorphous form without showing crystalline peaks. The diffraction peaks show small amount of impurities of magnetite  $\text{Fe}_3\text{O}_4$  and Quartz. The XRD pattern of DCNC shows that  $\text{CoFe}_2\text{O}_4$  is successfully compounded with diatomite.



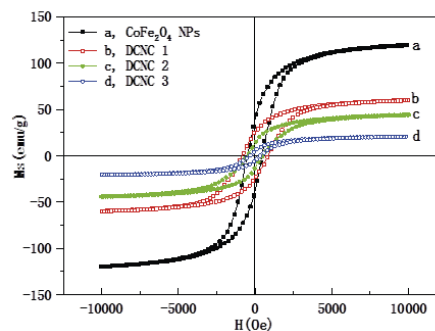
1. ábra FE-SEM EDX és TEM képekkel a  $\text{CoFe}_2\text{O}_4$  NP-k és a  $\text{CoFe}_2\text{O}_4$  NP-k DCNC-vel, a diatomit aránya 1: 10.  $\text{CoFe}_2\text{O}_4$  NP (a, e), DCNC (b, f). FESEM képek (a, b), FESEM-EDX a  $\text{CoFe}_2\text{O}_4$  NP-ről (c), DCNC (d). TEM képek (e, f)  
 Fig. 1 FE-SEM with EDX and TEM images of  $\text{CoFe}_2\text{O}_4$  NPs and DCNC with  $\text{CoFe}_2\text{O}_4$  NPs to diatomite ratio of 1 to 10.  $\text{CoFe}_2\text{O}_4$  NPs (a, e), DCNC (b, f). FESEM images (a, b), FESEM-EDX patterns of  $\text{CoFe}_2\text{O}_4$  NPs (c), DCNC (d). TEM images (e, f)



2. ábra A  $\text{CoFe}_2\text{O}_4$ NP-k, a diatomit és a DCNC XRD mintái, a  $\text{CoFe}_2\text{O}_4$  NP-k 1-10 közötti diatomit arányokkal  
 Fig. 2 XRD patterns of  $\text{CoFe}_2\text{O}_4$  NPs, diatomite and DCNC with  $\text{CoFe}_2\text{O}_4$  NPs to diatomite ratios of 1 to 10

### 3.3 Magnetic properties

$\text{CoFe}_2\text{O}_4$  NPs is a kind of widely used magnetic nanomaterial with large ferromagnetic anisotropy constants. Its magnetic properties originated from the magnetic coupling interaction between  $\text{Co}^{2+}$  and  $\text{Fe}^{3+}$  ions through oxygen atoms [25, 26]. The magnetic hysteresis loops of all samples were measured by VSMat room temperature (Fig. 3). Magnetic parameters of  $\text{CoFe}_2\text{O}_4$  NPs and DCNC such as coercivity (Hc), saturation magnetization (Ms), retentivity and Remanence ratio (Mr/Ms) are presented in Table 1.



3. ábra A  $\text{CoFe}_2\text{O}_4$  NP és DCNC mágnesezési görbéi. DCNC 1 és DCNC 3  $\text{CoFe}_2\text{O}_4$ NP-ekkel, a diatomit aránya 1:2, 1:5, illetve 1:10 között  
 Fig. 3 Magnetization curves of  $\text{CoFe}_2\text{O}_4$  NPs and DCNC. DCNC 1 to DCNC 3 with  $\text{CoFe}_2\text{O}_4$  NPs to diatomite ratios of 1 to 2, 1 to 5 and 1 to 10, respectively

| Samples                       | Coercivity Hc (Oe) | Saturation magnetization Ms (emu.g <sup>-1</sup> ) | Retentivity Mr (emu.g <sup>-1</sup> ) | Remanence ratio Mr/Ms |
|-------------------------------|--------------------|--|---------------------------------------|-----------------------|
| $\text{CoFe}_2\text{O}_4$ NPs | 837.07             | 96.5   | 49.9                                  | 0.52                  |
| DCNC 1                        | 262.07             | 53.43  | 10.94                                 | 0.2                   |
| DCNC 2                        | 148.21             | 43.39  | 6.04                                  | 0.14                  |
| DCNC 3                        | 403.07             | 32.61  | 9.08                                  | 0.28                  |

1. táblázat VSM-rel mért mágneses paraméterek  $\text{CoFe}_2\text{O}_4$  NP-k, DCNC 1 és DCNC 3,  $\text{CoFe}_2\text{O}_4$ NP-k, diatomit arányaránya 1:2, 1: 5, illetve 1:10 között  
 Table 1 Magnetic parameters measured from VSM for  $\text{CoFe}_2\text{O}_4$  NPs, DCNC 1 to DCNC 3 with  $\text{CoFe}_2\text{O}_4$  NPs to diatomite ratios of 1 to 2, 1 to 5 and 1 to 10, respectively

The hysteresis graphs for  $\text{CoFe}_2\text{O}_4$  NPs and DCNC are typical of the soft magnetic material.  $\text{CoFe}_2\text{O}_4$  NPs exhibits significant ferromagnetic behavior with Hc of 837.07Oe, Ms of 96.5 emu.g<sup>-1</sup>, Mr of 49.9 and Mr/Ms of 0.52. It seems that existing strong ferromagnetic coupling among  $\text{CoFe}_2\text{O}_4$  NPs, in which they ferromagnetically coupled together and behaving as magnetic nanochains rather than as individual NP [17]. As shown in Fig. 3, it is clear that the saturation magnetization of DCNC is much lower than the corresponding value of  $\text{CoFe}_2\text{O}_4$  NPs. Lower saturation magnetization is contributed to the addition of non-magnetic diatomite to  $\text{CoFe}_2\text{O}_4$  NPs. Therefore, from the aspect of engineering application, the magnetic properties of DCNC can be adjusted to meet the requirement of actual design by changing the compositions between diatomite and  $\text{CoFe}_2\text{O}_4$  NPs.

### 3.4 Dielectric properties

The microwave dielectric properties of  $\text{CoFe}_2\text{O}_4$  NPs and DCNC were measured at frequencies (0-18 GHz) by the microwave network analyzer. The electromagnetic properties are mainly characterized by two basic parameters<sup>[4, 27]</sup> as described by Eq.(1) and Eq.(2):

$$\text{Complex permittivity, } \epsilon_r = \epsilon' + i\epsilon'' \quad (1)$$

$$\text{Complex magnetic permeability, } \mu_r = \mu' + i\mu'' \quad (2)$$

Where  $\epsilon'$  and  $\epsilon''$  are the real part or dielectric constant and imaginary part or dielectric loss of the complex dielectric permittivity. Where  $\mu'$  and  $\mu''$  are the real magnetic permeability and magnetic loss.

In addition, the dielectric loss tangent (tan  $\delta$ ) characterizes the dielectric loss of a dielectric material after applying an

electric field. Where  $\delta$  is dielectric loss angle. The electric loss tangent is determined by the complex permittivity:

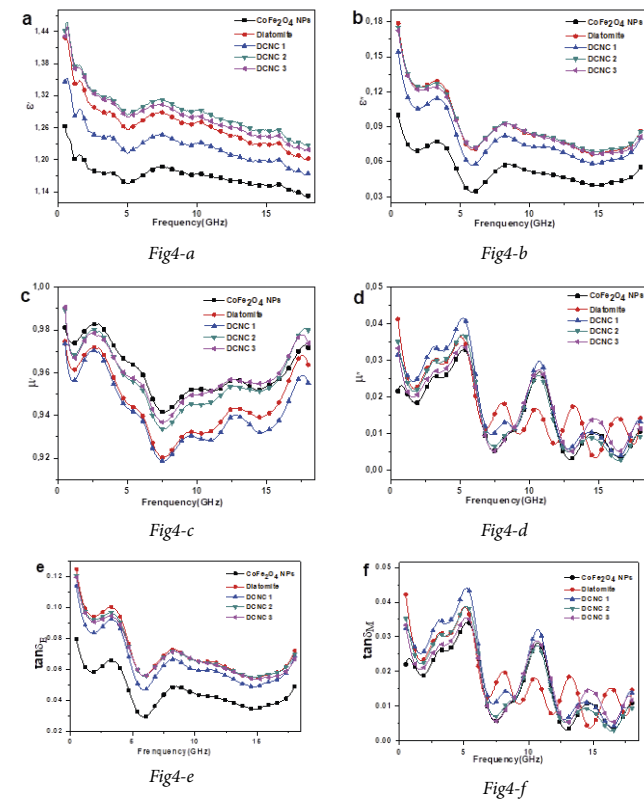
$$\tan \delta_E = \frac{\epsilon''}{\epsilon'} \quad (3)$$

The magnetic loss tangent is determined by the complex permeability:

$$\tan \delta_M = \frac{\mu''}{\mu'} \quad (4)$$

### 3.4.1 Dielectric properties

It is well known that the dielectric constant is the expression of the polarization capacity of the material. Dipoles, interfaces, ions and electron polarization favor dielectric loss. At lower frequencies, dipole and interfacial polarization are important for dielectric loss. However, ion and electron polarization make a most significant contribution to the dielectric loss at higher frequency [28]. Polarization and variation of dielectric constant in  $\text{CoFe}_2\text{O}_4$  and its complexes may be related to changes of  $\text{Fe}^{2+}$  and  $\text{Fe}^{3+}$  concentrations [29]. Moreover, the dielectric constant of  $\text{CoFe}_2\text{O}_4$  and its complexes depends on the amount of  $\text{Fe}^{2+}$  in the microwave frequency because they are susceptible to polarization than  $\text{Fe}^{3+}$  [30].



4. ábra A  $\text{CoFe}_2\text{O}_4$  NP-k, a diatomit és a DCNC dielektromos tulajdonságai. DCNC 1 és DCNC 3  $\text{CoFe}_2\text{O}_4$  NP-k, a diatomit aránya 1:2, 1:5, illetve 1:10 között. Komplex permittivitás ( $\epsilon$ , a, b), komplex permeabilitás ( $\mu$ , c, d) és veszteségtangens ( $\tan \delta$ , e, f). Az  $\epsilon'$  ( $\epsilon'$ , a) valódi része, az  $\epsilon''$  ( $\epsilon''$ , b) képzetes része.  $\mu'$  ( $\mu'$ , c) valódi része,  $\mu''$  ( $\mu''$ , d) képzetes része. Elektromos veszteségtangens ( $\tan \delta_E$ , e), mágneses veszteségtangens ( $\tan \delta_M$ , f)

Fig. 4 Dielectric properties of  $\text{CoFe}_2\text{O}_4$  NPs, diatomite and DCNC. DCNC 1 to DCNC 3 with  $\text{CoFe}_2\text{O}_4$  NPs to diatomite ratios of 1 to 2, 1 to 5 and 1 to 10, respectively. Complex permittivity ( $\epsilon$ , a, b), complex permeability ( $\mu$ , c, d) and loss tangent ( $\tan \delta$ , e, f). Real part of  $\epsilon$  ( $\epsilon'$ , a), imaginary part of  $\epsilon$  ( $\epsilon''$ , b). Real part of  $\mu$  ( $\mu'$ , c), imaginary part of  $\mu$  ( $\mu''$ , d). Electric loss tangent ( $\tan \delta_E$ , e), magnetic loss tangent ( $\tan \delta_M$ , f)

The dielectric properties of  $\text{CoFe}_2\text{O}_4$  NPs, diatomite and DCNC are shown in Fig. 4 in the frequency range of 2~18GHz. The  $\epsilon'$  of the samples always show a rapid decline and then a small increase, and finally a downward trend.  $\epsilon''$  appears to fall and then rise and then fall again, finally in rising trend. At 4~6Hz, 7~9Hz Fig. 4a and Fig. 4b appear more obvious dielectric resonance peak. The values of  $\epsilon'$ ,  $\epsilon''$  in single  $\text{CoFe}_2\text{O}_4$  are the smallest in the range of 2~18Hz. The value of  $\epsilon'$  fluctuates between 1.26~1.13 and the value of  $\epsilon''$  fluctuates in the range of 0.09~0.18. With the decrease in the mixing ratio of  $\text{CoFe}_2\text{O}_4$  and diatomite, the values of  $\epsilon'$ ,  $\epsilon''$  have been significantly improved. When the ratio of  $\text{CoFe}_2\text{O}_4$  to diatomite is 1:5, the values of  $\epsilon'$ ,  $\epsilon''$  are the largest and the best. The maximum values of  $\epsilon'$ ,  $\epsilon''$  are 1.47 and 0.18 respectively, and the minimum values are about 1.23 and 0.09 respectively. The peaks in the range of 4~6Hz are about 1.29 and 0.075 respectively, and the peaks in 7~9Hz are about 1.32 and 0.1. Significant relaxation peaks appeared at around 6 GHz and 15 GHz, indicating that there is dielectric relaxation in both  $\text{CoFe}_2\text{O}_4$  NPs and composites [31] and the polarization is strong. But only when  $\text{CoFe}_2\text{O}_4$  and diatomite ratio of 1:5 and 1:10, The values of  $\epsilon'$ ,  $\epsilon''$  are greater than a single diatomite and the effect is better after compositing. Although the composite of 1:10 is relatively smaller than that of 1:5, it is relatively close to that of 1:5. The maximum value of  $\epsilon'$  is about 1.44 and the minimum value is about 1.22 when the ratio of  $\text{CoFe}_2\text{O}_4$  to diatomite is 1:10. And its peaks in 4~6Hz and 7~9Hz are about 1.29 and 1.31 respectively. Its value of  $\epsilon''$  is almost the same to the value of 1:5, so it is more economical in practical application. And when  $\text{CoFe}_2\text{O}_4$  and diatomite ratio is 1:2, the values of  $\epsilon'$ ,  $\epsilon''$  are between single  $\text{CoFe}_2\text{O}_4$  and single diatomite. Thus, the effect is general. The loss tangent represents the loss of the microwave absorbing material and supports the dominant contribution of conductivity to dielectric loss. It can be seen from the Fig. 4e that the value of a single diatomite is the largest and the value of single  $\text{CoFe}_2\text{O}_4$  is the smallest, which is mainly because diatomite is a dielectric loss material and  $\text{CoFe}_2\text{O}_4$  is electromagnetic loss material. As the ratio of  $\text{CoFe}_2\text{O}_4$  to diatomite decreases, the loss tangent is also reduced.

### 3.4.2 Permeability properties

In the range of 2~18Hz, the values of  $\mu'$  of each sample shows a trend of decreasing at first and then rising, and fluctuating in a small range. The value of  $\mu''$  has a more complex change with a greater degree fluctuating. The value of  $\mu'$  of a single  $\text{CoFe}_2\text{O}_4$  is the largest in the range of 2~18Hz and the maximum is about 0.045, which is close to the ratio of  $\text{CoFe}_2\text{O}_4$  to diatomite at 1:10. However, as the ratio of  $\text{CoFe}_2\text{O}_4$  to diatomite increases, the value of  $\mu'$  decreases at the same frequency. When the ratio of  $\text{CoFe}_2\text{O}_4$  to diatomite is 1:2, the value of  $\mu'$  is the smallest in the range of 2~18Hz and the minimum is about 0.02. The single diatomite is slightly larger than it. In addition, the value of  $\mu''$  is the largest in the low frequency range whose maximum is about 0.045 but the single diatomite is the smallest and its minimum is about 0.015. In the high frequency range, the volatility is more complicated. The single diatomite is the largest in 12~14Hz and 16~18Hz and the peaks are about 0.023 and 0.015 respectively. Moreover, in 14~16Hz, the largest value

is 0.015 when the ratio of  $\text{CoFe}_2\text{O}_4$  to diatomite is 1:10. It can be seen from Fig. 4d that the magnetic permeability fluctuates greatly with frequency, and multiple resonance peaks appear, indicating the presence of ferromagnetic resonance behavior [32]. Due to the influence of  $\text{CoFe}_2\text{O}_4$  spinel structure on the anisotropy field, the magnetic field anisotropy causes a large change in magnetic permeability. The main source is that the unpaired electrons in the ferromagnetic medium use magnetic materials to absorb energy from the microwave magnetic field and cause magnetic energy loss. According to the analysis of magnetic loss tangent, in the low frequency range, the loss is the largest when the ratio of  $\text{CoFe}_2\text{O}_4$  to diatomite is 1:2 and the performance is closer when the ratio of  $\text{CoFe}_2\text{O}_4$  to diatomite is 1:5 and 1:10. In the High-frequency range, the ratio of  $\text{CoFe}_2\text{O}_4$  to diatomite is 1:10 better than 1:5, and the loss angle tangent is greater.

In general, when the dielectric and magnetic properties of the composites are matched with each other, the microwave absorption effect will be better. Considering the economic rationality and the absorbing effect, when the ratio of  $\text{CoFe}_2\text{O}_4$  to diatomite is 1:10, the dielectric dissipation effect of diatomite and the magnetic dissipation effect of  $\text{CoFe}_2\text{O}_4$  NPs can be combined to achieve the best absorbing properties.

### 3.4.3 Microwave absorption properties

As shown in Fig. 5, the microwave absorption performances of the samples are basically the same, which have the best absorption effect when nearing 11 GHz. This phenomenon is consistent with the above analysis of the permeability. The porous structure of the diatomite as the matrix causes the electromagnetic wave traveling path to cause the formation of multiple internal reflections and multiple scattering, which significantly enhances the attenuation capability, thereby contributing to the enhancement of microwave absorption performance [33]. When the ratio of  $\text{CoFe}_2\text{O}_4$  to diatomite is 1:2, the composite has the best absorbing effect. When the ratio of  $\text{CoFe}_2\text{O}_4$  to diatomite is 1:10 and 1:5, the wave absorbing performance is the second. The peak is about -9dB in 4~6Hz. The range of <10Hz is between 10Hz and 12Hz and the maximum reflection loss is about -12dB. In addition, when the ratio of  $\text{CoFe}_2\text{O}_4$  to diatomite is 1:10, the composite has the best absorbing effect whose maximum reflection loss is about -9dB ranging from 12 to 18Hz, while the maximum reflection loss of other materials is only about -7Hz. As shown in Table 2, it reflects the maximum reflectivity loss for each material. From the economic point of view, when the ratio of  $\text{CoFe}_2\text{O}_4$  to diatomite is 1:10, the absorbing performance is close to that of  $\text{CoFe}_2\text{O}_4$  and diatomite of 1:2 in the low frequency range. Moreover, in the high frequency range, the composite of 1:10 has the best absorption effect.

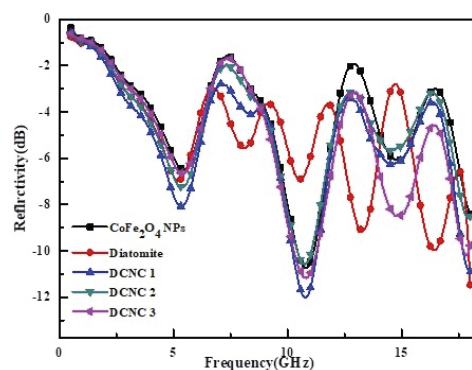
Therefore, the composite of 1:10 is most conducive to the promotion. It is worth noting that  $\text{CoFe}_2\text{O}_4$  and its complex have two secondary absorption peaks near the 5 GHz and 15 GHz frequencies, which correspond to the minimum value of the sample loss tangent rather than the sub-peak corresponding to the loss tangent. The absorption peak has moved. In a word, the absorbing ability of the material is not only closely related to its permeability, but also has a significant relationship with

the thickness of the absorbing plate, which will result in the left and right offset of peak positions of absorption peaks and values of loss tangent. Therefore, the wide peak value of the loss tangent will be of great importance to the expansion of absorbing capacity, so that the material can meet the requirements of multi-band and various thicknesses.

| Sample                        | Maximum reflectivity loss/dB | The corresponding frequency/Hz |
|-------------------------------|------------------------------|--------------------------------|
| $\text{CoFe}_2\text{O}_4$ NPs | 10.73                        | 10.83                          |
| Diatomite                     | 8.42                         | 18                             |
| DCNC 1                        | 12.04                        | 10.74                          |
| DCNC 2                        | 10.59                        | 10.74                          |
| DCNC 3                        | 11.17                        | 10.83                          |

2. táblázat A  $\text{CoFe}_2\text{O}_4$  NP-k, a diatomit és a DCNC maximális reflexiós vesztesége. DCNC 1 és DCNC 3  $\text{CoFe}_2\text{O}_4$ NP-k, a diatomit aránya 1:2, 1:5, illetve 1:10 között

Table 2 The maximum reflectivity loss of  $\text{CoFe}_2\text{O}_4$  NPs, diatomite and DCNC. DCNC 1 to DCNC 3 with  $\text{CoFe}_2\text{O}_4$  NPs to diatomite ratios of 1 to 2, 1 to 5 and 1 to 10, respectively



5. ábra A  $\text{CoFe}_2\text{O}_4$  NP-k, a diatomit és a DCNC mikrohullámú abszorpciós tulajdonságai. DCNC 1 és DCNC 3  $\text{CoFe}_2\text{O}_4$ NP-kkel, a diatomit aránya 1: 2, 1:5, illetve 1:10 között

Fig. 5 Microwave absorption properties of  $\text{CoFe}_2\text{O}_4$  NPs, diatomite and DCNC. DCNC 1 to DCNC 3 with  $\text{CoFe}_2\text{O}_4$  NPs to diatomite ratios of 1 to 2, 1 to 5 and 1 to 10, respectively

## 4. Conclusions

In summary, the DCNC of  $\text{CoFe}_2\text{O}_4$ /diatomite were fabricated via citric acid-nitrate sol-gel auto-combustion method. The FE-SEM and TEM observations confirmed that the magnetic NPs were uniformly dispersed in the surface and porous structure of diatomite to form stable DCNC. Magnetic measurements show that all samples are ferromagnetic, and that the  $\text{Co}^{2+}$  occupies the octahedral (B) site, will result in a reduction in the A-O-B super exchange interaction and a total of the magnetic properties of  $\text{Fe}^{3+}$  ions reduce. The microwave dielectric properties of the DCNC show that the dielectric and magnetic properties of the composites are optimized. The optimized best absorption performance of DCNC with ratio of  $\text{CoFe}_2\text{O}_4$  to diatomite is 1:10 considering the economic rationality and the absorbing performances. In generally, our study shows a promising way for construction of diatomite-based functional nanomaterials.

## 5. Acknowledgements

This work was supported by the National Natural Science Foundation of China (NSFC, Nos. 42011530085, 41672039), Russian Foundation for Basic Research (RFBR, No. 20-55-53019), the Sichuan Science and Technology Program (2019JDJQ0056), and the Longshan Academic Talent Research Support Program of the Southwest University of Science and Technology (18LZX405).

## References

- [1] Cao, S. – Ding, Y. – Yang, M. – Pan, H.: Lightweight and nitrogen-doped graphene nanoribbons with tunable hierarchical structure for high performance electromagnetic wave absorption. *Ceramics International*, 2018; 44(16): 20259-20266.
- [2] Deniz, Ö. G. – Kıvrak, E. G. – Kaplan, A. A. – Altunkaynak, B. Z.: Effects of folic acid on rat kidney exposed to 900 MHz electromagnetic radiation. *Journal of Microscopy & Ultrastructure*, 2017; 5(4): 198-205.
- [3] Gandhi, N. – Singh, K. – Ohlan, A. – Singh, D. P.: Thermal, dielectric and microwave absorption properties of polyaniline-CoFe<sub>2</sub>O<sub>4</sub> nanocomposites. *Composites Science & Technology*, 2011; 71(15): 1754-1760.
- [4] Moradmard, H. – Shayesteh, S. F. – Tohidi, P. – Abbas, Z.: Structural, magnetic and dielectric properties of magnesium doped nickel ferrite NPs. *Journal of Alloys and Compounds*, 2015; 650: 116-122.
- [5] Lenin, N. – Sakthipandi, K. – Kanna, R. R. – Rajkumar, G.: Electrical, magnetic and structural properties of polymer-blended lanthanum-added nickel nano-ferrites. *Ceramics International*, 2018; 44(17): 21866-21873.
- [6] Wen, B. – Cao, M. – Lu, M. – Cao, W.: Reduced graphene oxides: light-weight and high-efficiency electromagnetic interference shielding at elevated temperatures. *Advanced Materials*, 2014; 26(21): 3484-3489.
- [7] Yuan, L. M. – Xu, Y. G. – Dai, F. – Liao, Y.: The microwave properties of composites including lightweight core-shell ellipsoids. *Journal of Magnetism and Magnetic Materials*, 2016; 419: 494-499.
- [8] Feng, A. – Jia, Z. – Zhao, Y. – Lv, H.: Development of Fe/Fe<sub>3</sub>O<sub>4</sub>@C composite with excellent electromagnetic absorption performance. *Journal of Alloys and Compounds*, 2018; 745: 547-554.
- [9] Yan, Z. Q. – Cai, J. – Xu, Y. G. – Zhang, D. Y.: Microwave absorption property of the diatomite coated by Fe-CoNiP films. *Applied Surface Science*, 2015; 346: 77-83.
- [10] O'Handley, R. C.: *Modern Magnetic Materials: Principles and Applications*. 2000.
- [11] Decurtins, S.: *Magnetic Materials. Fundamentals and Device Applications*. Von Nicola Spaldin. *Angewandte Chemie International Edition*, 2003; 42(47): 5791-5791.
- [12] Zhao, D. – Wu, X. – Guan, H. – Han, E.: Study on supercritical hydrothermal synthesis of CoFe<sub>2</sub>O<sub>4</sub> NPs. *Journal of Supercritical Fluids*, 2007; 42(2): 226-233.
- [13] Zhang, S. – Jiao, Q. – Zhao, Y. – Li, H.: Preparation of rugby-shaped CoFe<sub>2</sub>O<sub>4</sub> particles and their microwave absorbing properties. *Journal of Materials Chemistry A*, 2014; 2(42): Accepted Manuscript, 18033-18039.
- [14] Wang, L. – Guan, Y. – Qiu, X. – Zhu, H.: Efficient ferrite/Co/porous carbon microwave absorbing material based on ferrite@metal-organic framework. *Chemical Engineering Journal*, 2017; 326: 945-955.
- [15] Yan, X. – Chen, J. – Xue, Q. – Miele, P.: Synthesis and magnetic properties of CoFe<sub>2</sub>O<sub>4</sub> NPs confined within mesoporous silica. *Microporous & Mesoporous Materials*, 2010; 135(1): 137-142.
- [16] Bagheri, M. – Bahrevar, M. A. – Beitollahi, A.: Synthesis of mesoporous magnesium ferrite (MgFe<sub>2</sub>O<sub>4</sub>) using porous silica templates. *Ceramics International*, 2015; 41(9, Part B): 11618-11624.
- [17] Liu, P. – Huang, Y. – Zhang, X.: Synthesis, characterization and excellent electromagnetic wave absorption properties of graphene@CoFe<sub>2</sub>O<sub>4</sub> @ polyaniline nanocomposites. *Synthetic Metals*, 2015; 201: 76-81.
- [18] Yang, H. – Ye, T. – Lin, Y. – Liu, M.: Preparation and microwave absorption property of graphene/BaFe<sub>12</sub>O<sub>19</sub>/CoFe<sub>2</sub>O<sub>4</sub> nanocomposite. *Applied Surface Science*, 2015; 357(3): 1289-1293.
- [19] Sun, Z. – Yao, G. – Liu, M. – Zheng, S.: In situ synthesis of magnetic MnFe<sub>2</sub>O<sub>4</sub>/diatomite nanocomposite adsorbent and its efficient removal of cationic dyes. *Journal of the Taiwan Institute of Chemical Engineers*, 2017; 71: 501-509.
- [20] Fu, W. – Liu, S. – Fan, W. – Yang, H.: Hollow glass microspheres coated with CoFe<sub>2</sub>O<sub>4</sub> and its microwave absorption property. *Journal of Magnetism & Magnetic Materials*, 2007; 316(1): 54-58.
- [21] Shen, W. – Ren, B. – Cai, K. – Song, Y-f.: Synthesis of nonstoichiometric Co<sub>0.8</sub>Fe<sub>2.2</sub>O<sub>4</sub>/reduced graphene oxide (rGO) nanocomposites and their excellent electromagnetic wave absorption property. *Journal of Alloys and Compounds*, 2019; 774: 997-1008.
- [22] Zha, Y. – Zhou, Z. – He, H. – Wang, T.: Nanoscale zero-valent iron incorporated with nanomagnetic diatomite for catalytic degradation of methylene blue in heterogeneous Fenton system. *Water Science and Technology*, 2016; 73(11): 2815-2823.
- [23] Yusan, S. – Korzhynbayeva, K. – Aytas, S. – Tazhibayeva, S.: Preparation and investigation of structural properties of magnetic diatomite nanocomposites formed with different iron content. *Journal of Alloys and Compounds*, 2014; 608: 8-13.
- [24] Dehestaniathar, S. – Khajelakzay, M. – Ramezani-Farani, M. – Ijadpanah-Saravi, H.: Modified diatomite-supported CuO-TiO<sub>2</sub> composite: Preparation, characterization and catalytic CO oxidation. *Journal of the Taiwan Institute of Chemical Engineers*, 2016; 58: 252-258.
- [25] Ayyappan, S. – Philip, J. – Raj, B.: Effect of Digestion Time on Size and Magnetic Properties of Spinel CoFe<sub>2</sub>O<sub>4</sub> NPs. *Journal of Physical Chemistry C*, 2009; 113(2): 590-596.
- [26] Manova, E. – Kunev, B. – Paneva, D. – Mitov, I.: Mechano-Synthesis, Characterization, and Magnetic Properties of NPs of Cobalt Ferrite, CoFe<sub>2</sub>O<sub>4</sub>. *Chemistry of Materials*, 2004; 16(26): 5689-5696.
- [27] Yusoff, A. N. – Abdullah, M. H. – Ahmad, S. H. – Jusoh, S. F.: Electromagnetic and absorption properties of some microwave absorbers. *Journal of Applied Physics*, 2002; 92(2): 876-882.
- [28] Kumar, A. – Sharma, P. – Varshney, D.: Structural, vibrational and dielectric study of Ni doped spinel Co ferrites: Co<sub>1-x</sub>Ni<sub>x</sub>Fe<sub>2</sub>O<sub>4</sub> (x = 0.0, 0.5, 1.0). *Ceramics International*, 2014; 40(8): 12855-12860.
- [29] Rezlescu, N. – Rezlescu, E.: Dielectric properties of copper containing ferrites. *Physica Status Solidi*, 2010; 23(2): 575-582.
- [30] Verma, A. – Saxena, A. K. – Dube, D. C.: Microwave permittivity and permeability of ferrite-polymer thick films. *Journal of Magnetism & Magnetic Materials*, 2003; 263(1): 228-234.
- [31] Liu, Z. – Xu, G. – Zhang, M. – Xiong, K.: Synthesis of CoFe<sub>2</sub>O<sub>4</sub>/RGO nanocomposites by click chemistry and electromagnetic wave absorption properties. *Journal of Materials Science Materials in Electronics*, 2016; 27(9): 1-8.
- [32] Liu, J. – Cao, M. S. – Luo, Q. – Shi, H. L.: Electromagnetic Property and Tunable Microwave Absorption of 3D Nets from Nickel Chains at Elevated Temperature. *ACS Applied Materials & Interfaces*, 2016; 8(34): 22615.
- [33] Jiang, L. – Liu, L. – Xiao, S. – Chen, J.: Preparation of a novel manganese oxide-modified diatomite and its aniline removal mechanism from solution. *Chemical Engineering Journal*, 2016; 284: 609-619.

### Ref.:

Huang, Haodong – He, Meng – Kotova, Olga B. – Golubev, Yevgeny – Dong, Faqin – Gömze, László A. – Kurovics, Emese – Lv, Rui – Sun, Shiyong: *Preparation and electromagnetic microwave adsorption performances of porous nanocomposite self-assembled by CoFe<sub>2</sub>O<sub>4</sub> nanoparticles and diatomite*  
Építőanyag – Journal of Silicate Based and Composite Materials, Vol. 72, No. 4 (2020), 124–129. p.  
<https://doi.org/10.14382/epitoanyag-jsbcm.2020.20>